Literature Cited

(1) Soliman, K. Doctoral dissertation, University of California, Santa Barbara, CA, 1987.
(2) McAllister, R. A. *AIChE J.* **1960**, *6*, 427.
(3) Dizechi, M.; Marschall, E. *J. Chem. Eng. Data* **1982**, *27*, 358.
(4) Dizechi, M. Doctoral dissertation, University of California, Santa Barbara, CA, 1980.
(5) O'Connor, T. Masters thesis, University of California, Santa Barbara, CA, 1983.

Received for review August 4, 1989. Revised March 1, 1990. Accepted May 29, 1990.

Measurements of the Critical Parameters and the Vapor–Liquid Coexistence Curve in the Critical Region of HCFC-123

Seisho Tanikawa,* Yasuo Kabata, Haruki Sato, and Koichi Watanabe

Department of Mechanical Engineering, Faculty of Science and Technology, Keio University, 3-14-1, Hiyoshi, Kohoku-ku, Yokohama 223, Japan

Measurements of the vapor–liquid coexistence curve in the critical region were made for HCFC-123 ($CHCl_2CF_3$) by visual observation of the vapor–liquid interface in an optical cell. Thirty densities of both saturated liquid and vapor were obtained in the range of temperatures from 401 K to the critical temperature corresponding to the density range between 203 and 1141 kg/m^3. The experimental uncertainty of the temperature measurements was estimated to be less than ±12 mK, while that of the density measurements was estimated to be between ±0.09% and ±0.53%. Not only the level where the meniscus disappeared but also the intensity of the critical opalescence were considered for the determination of the critical temperature T_c and the critical density ρ_c of HCFC-123 as 456.86 ± 0.02 K and 556 ± 3 kg/m^3, respectively. The critical exponent β was also determined, and the correlation of the saturated liquid density of HCFC-123 was established.

Introduction

HCFC-123 (2,2-dichloro-1,1,1-trifluoroethane, $CHCl_2CF_3$) attracts a great deal of attention as a stratospherically safe alternative to CFC-11 (trichlorofluoromethane, CCl_3F), which is mainly used as a blowing agent and as a refrigerant for turbo-refrigeration machines. A comparison of some general physicochemical properties of HCFC-123 with CFC-11 is shown in Table I. The critical parameters are essential and important in predicting various thermodynamic properties and in formulating equations of state. By means of visual observation of the meniscus in an optical cell, the critical temperature and the critical density of HCFC-123 were determined. The level where the meniscus disappeared and the intensity of the critical opalescence observed were the key factors for determining the critical parameters of HCFC-123. Because of its high critical temperature, we modified our original apparatus (*1*) so as to perform accurate measurements at even higher temperatures beyond 425 K.

The saturated liquid densities and saturated vapor densities near the critical point were also determined by the observing disappearance of the meniscus in the cell. The critical exponent β and the saturated liquid density correlation were subsequently determined on the basis of the present measurements with available other data.

* To whom correspondence should be addressed.

Table I. General Properties of CFC-11 and HCFC-123[a]

substance	CFC-11	HCFC-123
chemical formula	CCl_3F	$CHCl_2CF_3$
molar mass, g/mol	137.368	152.931
critical temperature, K	471.15	456.86*
critical pressure, MPa	4.409	3.6655
critical density, kg/m^3	554	556*
critical volume, cm^3/mol	248	275
normal boiling point, K	297	301.5
freezing point, K	162	172
dipole moment, D	0.5	
ozone depletion potential	1.0	<0.05
global warming potential	0.4	<0.1

[a] Values marked with an asterisk were determined in the present work.

Experimental Section

The experimental apparatus and basic experimental procedures have been already described in the previous papers (*1–3*). By using the apparatus, we have already measured critical properties of HFC-23 (*1*), CFC-12 (*2*), HCFC-22 (*2*), Halon-1301 (*3*), CFC-114 (*4*), HFC-152a (*5*), CFC-115 (*6*), HFC-134a (*7*), and azeotropic mixture refrigerant 502 (*8*), respectively. The apparatus is composed of three vessels, i.e., an optical cell with two synthetic sapphire windows (15 mm in thickness) for observing the meniscus behavior of the sample fluid, an expansion vessel, and a supplying vessel.

In this study, two modifications were made for performing the measurements of HCFC-123. Firstly, we constructed new vessels so as to perform measurements at higher temperatures beyond 425 K. A new optical cell is shown in Figure 1. A gold packing (0.2 mm in thickness) and an aluminum packing (1 mm in thickness) between a sapphire window and the cell made of 304 stainless steel were used for the high-temperature sealing. The other two vessels made of 304 stainless steel were designed so as to withstand higher temperatures and pressures. These vessels were connected to high-temperature and -pressure valves (Sno-Trik Model SS-410-FP). The inner volumes of the respective three vessels were calibrated by using pure water, because its density value at room temperature (298.15 K) is well-known. The volumes are 10.956 ± 0.004, 6.249 ± 0.004, and 77.305 ± 0.004 cm^3, respectively.

Secondly, a new expansion procedure called "supplementary expansion" was introduced so as to improve the accuracy and ease of determining the various density values. This expansion procedure makes it possible to make subtle density changes for the measurements in the high-density region.

0021-9568/90/1735-0381$02.50/0

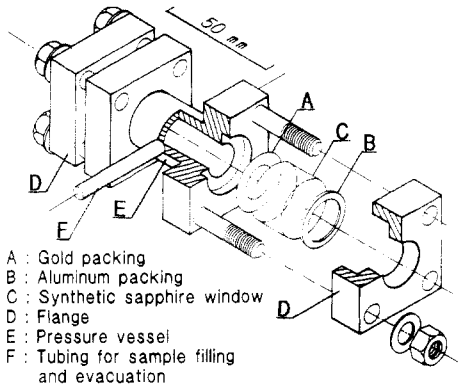

Figure 1. New optical cell.

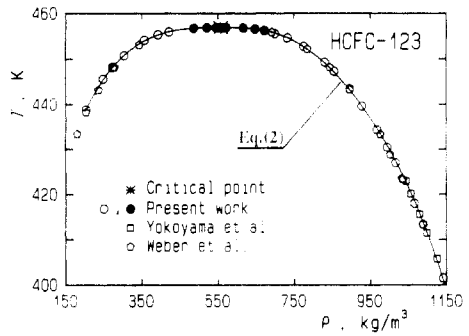

Figure 2. Coexistence curve of HCFC-123 in the critical region.

The main part of the apparatus was installed in a thermostated bath where heat-transfer medium was filled and stirred. For selection of the heat-transfer medium, high thermal stability, low viscosity, nontoxicity, and transparency have to be considered. Particularly, the transparency is essential in the present study to observe small changes in the color and the intensity of the critical opalescence near the critical point. We selected perfluoropolyethers (Montefluos, Y-25) because of its excellent transparency characteristics at temperatures up to 500 K.

The temperature measurements were conducted with a 25-Ω platinum resistance thermometer, which was placed at the vicinity of the optical cell. The thermometer was calibrated according to IPTS-68 at the National Research Laboratory of Metrology, Tsukuba, Japan. The bath temperature was controlled automatically within ±7 mK with the aid of a PID temperature controller. We measured four different HCFC-123 samples. The purities were 99.8, 99.82, 99.93, and 99.99 wt %, respectively.

Results

In the critical region from 401.5 K to the critical temperature ($0.88 < T_r$) corresponding to densities between 203 and 1141 kg/m³ ($0.37 < \rho_r < 2.05$), 19 saturated liquid densities and 11 saturated vapor densities of HCFC-123 were obtained. The experimental results are shown in Table II. The uncertainty of the temperature measurements depends upon the fluctuation of the thermostated bath temperature, the reliability of the thermometer, and the individual error with respect to the determination of the meniscus-disappearing temperature. The uncertainty of the temperature measurements is estimated to be less than ±12 mK. The uncertainty of the density measurements depends upon the number of expansion procedures, being between ±0.09% and ±0.53%, as shown in Table II. Figure 2 shows the present results on a temperature–density diagram, together with saturated densities above 400 K measured by Yokoyama et al. (*9*) and Weber et al. (*10*). The present results for the saturated liquid density except for those in the vicinity of the critical point are in good agreement with

Table II. Densities of the Saturated Vapor (ρ'') and Liquid (ρ') for HCFC-123[a]

T, K	ρ'', kg/m³	T, K	ρ', kg/m³
438.81_9	203.4 ± 0.5[b]	456.85_5	556.4 ± 0.5*[c]
445.55_8	248.6 ± 0.4[b]	456.86_0	559.6 ± 0.5*[c]
448.10_2	272.3 ± 1.4[b]	456.83_3	569.9 ± 1.8*[d]
450.75_3	303.9 ± 0.3[b]	456.75_3	614.9 ± 1.9*[e]
454.08_3	356.4 ± 1.1[c]	456.51_9	645.9 ± 2.3*[e]
455.33_0	391.6 ± 2.0[e]	456.17_3	671.2 ± 0.6*[e]
455.91_2	420.4 ± 0.4[b]	455.52_6	698.9 ± 1.1[c]
456.71_1	485.3 ± 1.0*[c]	454.55_6	732.1 ± 1.2[d]
456.82_4	519.6 ± 0.8*[c]	452.67_9	775.0 ± 2.0[e]
456.86_4	544.1 ± 1.7*[c]	449.20_8	830.0 ± 1.7[e]
456.87_0	554.6 ± 0.5*[c]	447.22_7	854.9 ± 0.8[c]
		443.36_3	895.6 ± 0.8[d]
		439.59_3	927.7 ± 2.3[e]
		434.34_2	966.7 ± 0.9[e]
		430.37_2	993.8 ± 1.9[e]
		426.94_5	1015.9 ± 1.4[e]
		417.96_7	1064.8 ± 1.5[e]
		413.30_1	1088.6 ± 1.0[e]
		401.50_7	1141.1 ± 1.0[e]

[a] For values marked with an asterisk, critical opalescence was observed. [b] 99.82 wt % purity HCFC-123. [c] 99.99 wt % purity HCFC-123. [d] 99.8 wt % purity HCFC-123. [e] 99.93 wt % purity HCFC-123.

the measurements by Yokoyama et al. and Weber et al. within experimental uncertainty. The present results of the saturated vapor density are slightly smaller than those of Weber et al. with the maximum difference of 4 kg/m³. The claimed uncertainty of the density measurements by Weber et al. is ±2 kg/m³ so that such a difference in the vapor densities is within the allowable limit of the experimental uncertainty of the measurements.

The critical opalescence was observed in 10 measurements in densities between 485.3 and 671.2 kg/m³ with corresponding temperatures above 0.70 K below the critical temperature. These measurements are given in Figure 2, being indicated with a solid circle, and in Table II, being indicated with an asterisk. The meniscus descended with increasing temperature and disappeared at the bottom of the optical cell 8 different densities between 203.4 and 485.3 kg/m³, while it ascended and disappeared at the top of the optical cell 16 densities between 614.9 and 1141.1 kg/m³. And the meniscus disappeared without reaching the top or bottom of the optical cell in 6 densities between 519.6 and 569.9 kg/m³. Notably, in 3 densities of 554.6, 556.4, and 559.6 kg/m³, the meniscus stayed at the same position, the center of the optical cell, and became indistinguishable with increasing temperature.

At the critical point, the meniscus disappears at the center of the optical cell and the critical opalescence is observed most intensely and equally in both the vapor and the liquid phases. The level where the meniscus disappeared and the intensity of the critical opalescence were principal criteria for the determination of the critical parameters. By judging from the level where the meniscus disappeared, it was clearly found that the critical density of HCFC-123 should exist between 544.1 and 569.9 kg/m³. Then, we measured three different densities of 554.6, 556.4, and 559.6 kg/m³ near the critical density. In the case of these three measurements, the most pure HCFC-123, 99.99 wt %, was used. The meniscus disappeared at the center of the optical cell in these three densities near the critical density. The obvious difference of the intensity in the critical opalescence was observed among these measurements. In the density of 554.6 kg/m³, the critical opalescence in the liquid phase was observed more intensely than it was in the vapor phase, while the critical opalescence in the vapor phase was observed more intensely than it was in the liquid phase in the density of 559.6 kg/m³, in the case of 556.4 kg/m³, the critical opalescence in the vapor phase was observed as being a little

Table III. Critical Parameters of HCFC-123

investigator(s)	year	T_c, K	P_c, MPa	ρ_c, kg/m^3	methods[a]
ICI(11)	1987	456	3.607		
Atwood(12)	1988	457.15	3.732	554	
Daikin Kogyo(13)	1988	459.5	3.874	540	
Weber et al.(10)	1989	456.87 ± 0.03	3.674 ± 0.004	550 ± 4	2,3,4
Kamimura et al.(14)	1990	456.94 ± 0.04	3.672 ± 0.004	553 ± 5	1,3
Present work	1989	456.86 ± 0.02		556 ± 3	1

[a] Methods: (1) disappearance of the meniscus; (2) disappearance and reappearance of the meniscus; (3) extrapolation of vapor-pressure correlation; (4) extrapolation of rectilinear diameter.

more intense than in the liquid phase. On the basis of these observations, we considered that the density of 556.4 kg/m^3 was the saturated liquid density but the closest density to the critical point among the present results.

In consideration of the meniscus behavior near the critical point, the critical density of HCFC-123 was determined finally as

$$\rho_c = 556 \pm 3 \text{ kg/m}^3$$

The critical temperature T_c was determined as the saturation temperature corresponding to the critical density. As shown in Table II, the temperature range corresponding to the density range between 544.1 and 559.6 kg/m^3 was coincident within the uncertainty range of the temperature measurements. The temperature corresponding to the density of 556.4 kg/m^3, the closest measured density to the critical density, was 456.855 K. Therefore, the critical temperature of HCFC-123 was determined as

$$T_c = 456.86 \pm 0.02 \text{ K}$$

Two interesting phenomena, which we have not observed in the case of CFC measurements, were observed in the case of HCFC-123 measurements. Firstly, at the densities of 556.4 and 554.6 kg/m^3, the critical opalescence was most intense at a temperature 20 mK higher than the meniscus-disappearing temperature and the strong scattering of the visible spectrum was observed. Another phenomenon is that the liquid phase of the sample turned slightly brown after a series of measurements over 100–180 h. We did not observe any significant difference among the measurements due to the difference of the sample purity, except in the vicinity of the critical point. In some measurements of densities between 520 and 580 kg/m^3, however, a very minute difference among saturation temperatures was observed due to the difference of the sample purity. So it is considered that a very small quantity of HCFC-123 or that some sort of impurities might be decomposed at higher temperatures.

Available information about the critical parameters of HCFC-123 is summarized in Table III. Among the values listed in Table III, only two of them, which are given by Kamimura et al. (*14*) and by Weber et al. (*10*), state how to obtain these values and the associated uncertainties. The present critical temperature is lower than that of Kamimura et al. by 0.10 K, but it is in very good agreement with the value of Weber et al., within respective uncertainties. With respect to the critical density, our result is also in good agreement with the values of Weber et al., within respective uncertainties. It should be noted that the present result has been achieved with the smallest uncertainty among the entries of Table III on the basis of careful observations with very small temperature fluctuation within ±7 mK over many hours.

Discussion

The critical exponent β is important for correlating the vapor–liquid coexistence curve in the critical region by means of the power law representation, i.e.,

$$(\rho' - \rho'')/2\rho_c = B|(T - T_c)/T_c|^\beta \quad (1)$$

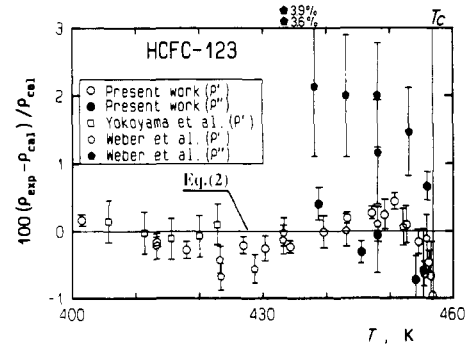

Figure 3. Deviations of the saturated vapor and liquid densities from eq 2.

where ρ', ρ'', T, ρ_c, T_c, and B denote saturated liquid density, saturated vapor density, temperature, critical density, critical temperature, and critical amplitude, respectively. A correlation of the vapor–liquid coexistence curve was established. The correlation of the vapor–liquid coexistence curve for HCFC-123 has the same expression as those for CFC-114 (*4*), HFC-152a (*5*), and HFC-134a (*7*) reported in our previous papers, i.e.,

$$\Delta\rho^* = -10.989|\Delta T^*|^{(1-\alpha)} + 19.417|\Delta T^*| - 11.538|\Delta T^*|^{(1-\alpha+\Delta_1)} \pm 1.7873|\Delta T^*|^\beta \pm 0.46103|\Delta T^*|^{(\beta+\Delta_1)} \quad (2)$$

where $\Delta\rho^* = (\rho - \rho_c)/\rho_c$, $\Delta T^* = (T - T_c)/T_c$, and α and β are critical exponents. The exponent Δ_1 stands for the first symmetric correction-to-scaling exponent in the Wegner expansion (*15*). From a theoretical background, these exponents are $\alpha = 0.1085$, $\beta = 0.325$, and $\Delta_1 = 0.50$ (*15*). The critical parameters in eq 2 determined in this study are $T_c = 456.86$ K and $\rho_c = 556$ kg/m^3. The coefficients in eq 2 were determined by least-squares fitting on the basis of the present results, except eight measurements between 485.3 and 614.9 kg/m^3 around the critical point that were excluded from the input data. The upper sign "+" and the lower sign "−" of the fourth and fifth terms in eq 2 correspond to the saturated liquid and vapor, respectively. This correlation is effective in a range of densities from 203 to 1141 kg/m^3. The saturation curve calculated from eq 2 is shown in Figure 2. The density deviation of the input data, together with the available data above 400 K, from eq 2 is shown in Figure 3. The deviations of the saturated liquid densities are shown by open symbols, while those for the saturated vapor densities are shown by solid symbols in Figure 3. Equation 2 reproduces 15 present liquid densities used as the input data with a standard deviation of 0.31% and 7 present vapor densities with a standard deviation of 0.45%. Concerning the available data by Weber et al., eq 2 represents 10 liquid densities with a standard deviation of 0.28% and 5 vapor densities with a standard deviation of 1.7%. Two measurements at 180.2 and 179.3 kg/m^3 were deviated by about 4% from eq 2 since these measurements are out of the effective range of eq 2.

Figure 4 shows a logarithmic plot between $(\rho' - \rho'')/2\rho_c$ and $|\Delta T^*|$ in terms of the present measurements and calculated results by eq 2. Open circles correspond to results of the liquid

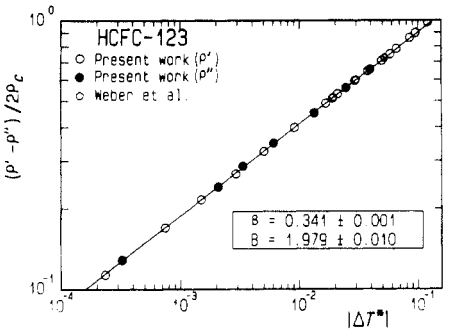

Figure 4. Relation between $(\rho' - \rho'')/2\rho_c$ and $|\Delta T^*|$.

densities, while solid circles to those of the vapor densities. The power law representation, eq 1, suggests that the experimental results can be fitted satisfactorily by a straight line and the slope is equivalent to the critical exponent β, as shown in Figure 4. For determination of the critical exponent β, 16 measured data in the range of the reduced temperature difference $3.3 \times 10^{-4} < |\Delta T^*| < 4.0 \times 10^{-2}$ were used. As a result of least-squares fitting, the values of β and B were obtained as follows:

$$\beta = 0.341 \pm 0.001$$

$$B = 1.979 \pm 0.010$$

As for HCFC-123, the value of the exponent β was greater than the theoretical value of 0.325 (*15*), but it is in a good agreement with the averaged value of $\beta = 0.337$ with respect to those of six refrigerants determined in our previous measurements (*7*). The measurements by Weber et al. are also shown in Figure 4, since some of the saturated liquid and vapor density measurements are performed at a common temperature. These plots also agree with the straight line being characterized with the critical exponent β mentioned above.

On the basis of our measurements and available saturated liquid density data reported by Yokoyama et al. (*9*), Maezawa et al. (*16*), and Weber et al. (*10*), a correlation of the saturated liquid density curve for HCFC-123 was developed as follows:

$$\Delta\rho^* = 1.8048|\Delta T^*|^{0.341} + 0.72872|\Delta T^*|^{0.68} + 0.34491|\Delta T^*|^{3.0} \quad (3)$$

where ΔT^* and $\Delta\rho^*$ are same as in eq 2. As the input data, 102 experimental data including 16 present measurements except the measurements in the vicinity of the critical point, 46 data by Yokoyama et al., 23 data by Maezawa et al., and 17 data by Weber et al. were used. The first exponent in eq 3 is the critical exponent $\beta = 0.341$, while other exponents have been determined by trial and error. The coefficients were determined by least-squares fitting. The effective range of eq 3 is in a temperature range from 200 K to the critical temperature. The deviation plots of the input data from eq 3 are shown in Figure 5. Equation 3 reproduces the present results, except those near the critical point, with a standard deviation of 0.07%, those by Maezawa et al. with 0.12%, those by Yokoyama et al. with 0.08%, and those by Weber et al. with 0.18%.

The saturated liquid correlations being effective up to the critical temperature have been reported by Maezawa et al. (*16*) and by Weber et al. (*10*). The correlation by Maezawa et al. has only two terms as a function of ΔT^*, and it established on the basis of their own data and the present data. The correlation by Weber et al. is represented with three-term expression as a function of ΔT^*, and it has been established on the basis of their own data. The comparison of eq 3 with the saturated liquid density correlations by Maezawa et al. and by Weber et al. is also shown in Figure 5. The correlation by Maezawa et al. agrees with the present correlation within the density deviation of ±0.2% at temperatures $T_r < 0.9$, except in the critical region where slightly larger deviations from the present result.

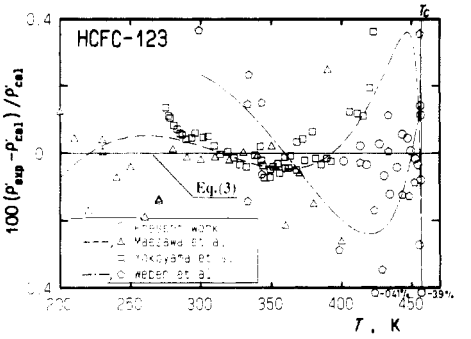

Figure 5. Deviations of the saturated liquid densities from eq 3.

The correlation by Weber et al. agrees well with the present correlation within ±0.2%, but in the vicinity of the critical point, however, it shows considerable discrepancy from eq 3 since the critical parameters included in their correlation are different from those adopted in the present work.

Conclusion

By means of visual observation of the meniscus in an optical cell, 30 saturated vapor and liquid densities of HCFC-123 in the critical region, the critical parameters, and the critical exponent β were determined. A saturated liquid density correlation for HCFC-123 was developed based on the present measurements with available other liquid density data. Our correlation is able to reproduce our data and other available data in the range of temperatures from 200 K to the critical temperature within their reported uncertainties.

Glossary

P	pressure, MPa
T	temperature, K
ρ	density, kg/m^3

Superscripts

$'$	saturated liquid
$''$	saturated vapor

Subscripts

c	critical point
r	reduced property

Literature Cited

(1) Okazaki, S.; Higashi, Y.; Takaishi, Y.; Uematsu, M.; Watanabe, K. *Rev. Sci. Instrum.* **1983**, *54*, 21.
(2) Higashi, Y.; Okazaki, S.; Takaishi, Y.; Uematsu, M.; Watanabe, K. *J. Chem. Eng. Data* **1984**, *29*, 31.
(3) Higashi, Y.; Uematsu, M.; Watanabe, K. *Bull. JSME* **1985**, *28*, 2660.
(4) Higashi, Y.; Uematsu, M.; Watanabe, K. *Bull. JSME* **1985**, *28*, 2969.
(5) Higashi, Y.; Ashizawa, M.; Kabata, Y.; Majima, T.; Uematsu, M.; Watanabe, K. *JSME Int. J.* **1987**, *30*, 1106.
(6) Kabata, Y. M.S. Thesis, Keio University, Yokohama, Japan, 1988.
(7) Kabata, Y.; Tanikawa, S.; Uematsu, M.; Watanabe, K. *Int. J. Thermophys.* **1989**, *10*, 605.
(8) Higashi, Y.; Uematsu, M.; Watanabe, K. *Int. J. Thermophys.* **1984**, *5*, 117.
(9) Yokoyama, C.; Takahashi, S. Preprint of the 29th High Pressure Conference of Japan, Fujisawa, Japan, 1988; p 116.
(10) Weber, L. A.; Levelt Sengers, J. M. H. *Fluid Phase Equilib.* **1990**, *55*, 241.
(11) ICI Chemical & Polymers Ltd. "ARCTON" 123 Preliminary Data Sheet, 1987.
(12) Atwood, T. *Int. J. Refrig.* **1988**, *11*, 234.
(13) Daikin Kogyo Co. Ltd. Daiflon 123 Data Sheet, 1988.
(14) Kamimura, T.; Watanabe, N.; Fukushima, M. Private communication from Asahi Glass Co., Ltd., Tokyo, 1990.
(15) Levelt Sengers, J. M. H.; Sengers, J. V. In *Perspectives in Statistical Physics*; Raveché, H. J., Ed.; North-Holland: Amsterdam, 1981; Chapter 14.
(16) Maezawa, Y.; Sato, H.; Watanabe, K. *J. Chem. Eng. Data* **1990**, *35*, 225.

Received for review August 22, 1989. Accepted May 15, 1990. We are greatly indebted to Asahi Glass Co., Ltd., Tokyo, Japan, for kindly furnishing

the sample fluid and perfluoro-polyethers, to E. I. du Pont de Nemours & Co., Wilmington, DE, for kindly furnishing the sample fluid, and to Shin-etsu Chemicals Co., Ltd., Tokyo, Japan, for furnishing the silicone oil. We are also greatly indebted to the National Research Laboratory of Metrology, Tsukuba, Japan, for the calibration of the thermometer. The assistance of Hitoshi Tanaka, who made elaborate observations with the present authors, is gratefully acknowledged. The financial support by the Grants-in-Aid for Scientific Research Fund in 1988-1989 (Project No. 63603024 and No. 01603022) by the Ministry of Education, Science and Culture, Japan, and the financial support by the Tokyo Electric Power Co., Inc., are gratefully acknowledged.

Viscosities of Poly(ethylene glycols)

Rong-Jwyn Lee and Amyn S. Teja*

School of Chemical Engineering, Georgia Institute of Technology, Atlanta, Georgia 30332-0100

Kinematic viscosities of the first six members of the poly(ethylene glycol) homologous series were measured at ambient pressure and several temperatures ranging from 293 to 423 K. A generalized correlation for the viscosity of poly(ethylene glycols) was also developed in terms of the number of carbon atoms. Excellent agreement was obtained between experimental and calculated viscosities.

Introduction

The poly(ethylene glycols) ($HOCH_2CH_2(OCH_2CH_2)_{n-1}OH$) have found a wide variety of applications in the automotive, pharmaceutical, petroleum, cosmetic, textile, and other industries. As a result, the measurement and correlation of their thermophysical properties have attracted a great deal of attention and effort. Gallaugher and Hibbert (*1*, *2*) reported the freezing point, vapor pressure, surface tension, and other physical properties of poly(ethylene glycols) and their derivatives. The thermal conductivity of the lower glycols was studied by Fischer (*3*), whereas Thomas et al. (*4*) and Bohne et al. (*5*) measured the viscosity of ethylene glycol. More recently, the density and thermal conductivity of the higher glycols were reported by Tawfik and Teja (*6*) and DiGuilio and Teja (*7*). Generalized correlations were also developed by these investigators. In the present study, we report the measurements of the viscosity of the first six members of the homologous series of poly(ethylene glycols) and develop a general correlation for the viscosity applicable to all members of the homologous series.

Experimental Section

Kinematic viscosities (ν) were measured by using a calibrated Cannon-Ubbelohde capillary viscometer made by International Research Glassware. According to Poiseuille's law, the kinematic viscosity is given by

$$\nu = C_1 t - C_2/t \qquad (1)$$

where t is the efflux time, and C_1 and C_2 are the viscometer constants. The correction due to kinetic energy, represented by C_2/t in the above expression, can generally be neglected if an appropriately sized viscometer is used, so that measurements of the kinematic viscosity can be obtained directly from the measurements of the efflux times. The viscometers were placed inside thermostated liquid baths in order to keep the temperature constant during the measurement. Two temperature baths, one filled with water and the other with oil, were used in this study. The water bath was used for low-temperature measurements, whereas the oil bath was used at high temperatures (beyond 350 K). The water-bath temperature could be held within ±0.03 K with use of a Haake recirculation temperature controller (Type E3). The oil-bath temperature was controlled by a Haake controller (Type D3) within ±0.1 K. Temperature measurement was done by a four-wire platinum resistance thermometer (YSI), which had previously been calibrated with a NBS calibrated standard platinum resistance thermometer (Leeds and Northrup Co., Serial No. 709892). The accuracy of the temperature measurement was estimated to be ±0.1 K. An electronic timer accurate to 1/100 s was used to obtain the efflux time.

Materials. Ethylene glycol (99.8%) and tri(ethylene glycol) (99.5%) were obtained from Fisher Scientific Co. Di(ethylene glycol) (99%), tetra(ethylene glycol) (99%), penta(ethylene glycol) (95%), and hexa(ethylene glycol) (98%) were obtained from the Aldrich Chemical Co. These chemicals were used as received.

Table I. Experimental Viscosities of Ethylene Glycol

this work			ref 4		ref 5	
T, K	ν, cSt	μ,[a] cP	T, K	ν, cSt	T, K	μ, cP
293.9	18.04	20.16	290.25	21.58	273.25	56.53
313.3	8.535	9.409	298.25	15.13	282.45	34.15
333.3	4.673	5.076	307.95	10.47	298.15	16.63
353.3	2.877	3.078	329.35	5.26	303.05	13.61
373.3	1.941	2.043	336.95	4.29	313.15	9.407
393.4	1.379	1.428	347.35	3.340	333.35	5.030
413.5	1.039	1.057	356.45	2.661	353.15	3.068
423.7	0.925	0.933	374.95	1.923	373.35	2.016
			383.25	1.645		
			392.75	1.426		
			404.25	1.206		
			413.85	1.053		
			422.75	0.940		
			433.05	0.831		

[a] The generalized density correlation of Tawfik and Teja was used.

Results and Discussion

The kinematic viscosity of ethylene glycol measured in this study is presented in Table I. Also listed in Table I are the literature values of Bohne et al. (*5*) and Thomas et al. (*4*), as well as absolute viscosities obtained by using the generalized density correlation of Tawfik and Teja (*6*). Excellent agreement was found between the three sets of data, with average absolute deviations (AAD) between our data and literature values being of the order of 1.0%. Viscosities of di-, tri-, tetra-, penta-, and hexa(ethylene glycols) are summarized in Table II. At least five samples were taken at each temperature to give the average values listed in these tables. The reproducibility of multiple samples was ±0.4%, and the accuracy of the data was estimated to be ±1.5%. A graphical representation of the

0021-9568/90/1735-0385$02.50/0